JOURNAL OF AIRCRAFT
Vol. 31, No. 5, Sept.–Oct. 1994

Recent Studies of Rotorcraft Blade-Vortex Interaction Noise

J. S. Preisser,* T. F. Brooks,† and R. M. Martin‡
NASA Langley Research Center, Hampton, Virginia 23665

Recent results are presented from several research efforts aimed at the understanding of rotorcraft blade-vortex interaction (BVI) in terms of the noise generation, directivity, and control. The results are based on work performed by NASA Langley Research Center researchers, both alone and in collaboration with other research organizations. Based on analysis of a simplified physical model, the critical parameters controlling BVI noise generation have been identified. The detailed mapping of the acoustic radiation field of a model rotor in a wind tunnel has revealed the extreme sensitivity of directivity to rotor advance ratio and disk attitude. The control and reduction of BVI noise through the use of higher harmonic pitch control is discussed.

Introduction

ROTOR blade-vortex interaction (BVI) noise, due to the interaction of a rotor blade with the tip vortices shed by preceding blades, has been a major topic of rotorcraft acoustic research for the past several years. BVI noise is intense, impulsive, and has frequency content in the midfrequency audible range, making it one of the most objectionable types of rotorcraft noise. Moreover, it is most likely to occur during low-speed rotorcraft descent, such as during approach for landing at heliports, which are often located in areas of high population.

The literature pertaining to BVI noise is broad and has involved many researchers from various organizations. Much of the work has been experimental. A comprehensive theory to accurately predict rotorcraft BVI noise generation and radiation is not yet available. Past experimental work in rotor BVI noise has attempted to define the operating regimes for its occurrence and the general direction of its radiation, utilizing both flight measurements[1–3] and wind-tunnel tests.[4–6] BVI noise has been found to be most intense in a direction forward of the rotor advancing side and downwards from the rotor plane.[1] Further experimental results have indicated that the more nearly parallel the tip vortex is to the blade at the time of interaction, the more intense the noise.[7] These previous tests were unfortunately limited by a small number of fixed measurement locations. Questions remained as to the sensitivity of radiation direction with changing advance ratio and tip-path plane angle, as well as to its controllability.

This article presents results from recent studies by NASA Langley Research Center researchers related to the understanding of BVI noise generation, radiation, and control. There is no intent in this article to assess the current state-of-the art in BVI. More complete discussions of a number of theoretical and experimental studies can be found in Refs. 8 and 9. This article focuses on results from a simplified physical analysis of the critical parameters controlling BVI,[10] and results from tests conducted in the German-Dutch acoustic wind tunnel (DNW)[11,12] and the Transonic Dynamics Tunnel (TDT) at NASA Langley.[13] The former test provided the first comprehensive set of data on BVI directional characteristics as a function of rotor advance ratio and disk attitude. The latter examined the effectiveness of higher harmonic pitch control for BVI noise reduction.

Blade-Vortex Interaction Noise Generation

Rotorcraft BVI is a highly complex, three-dimensional, time-dependent phenomena. As the rotor blades rotate, vorticity is continuously shed from the tip of each blade, due to the pressure difference between the upper and lower surfaces of each lifting blade. The vorticity rapidly rolls up, generating spiraling tip vortices whose paths depend on the rotational speed, forward speed, and the orientation of the rotor disk to the flight direction. In general, the vortex path is downward away from the rotor plane because of the rotor downflow, and thus does not ordinarily interact strongly with the rotor blades. However, under many operating conditions, such as hover and rotor descent at slow to moderate forward speed, the tip vortex paths intersect the rotor disk plane, generating impulsive loading on the blade that results in noise. A schematic illustrating the complexity of the BVI process for a four-bladed rotor system is shown in Fig. 1. The blade on the advancing first quadrant of the rotor undergoes multiple interactions due to the tip vortices of the blades 180 and 270 deg ahead. This situation is typical for moderate to high rotorcraft forward speeds. Lower speeds would produce more interactions due to the increased number of vortices present in the rotor plane. The blade near the top of the figure illustrates an interaction at a nearly normal angle to the blade

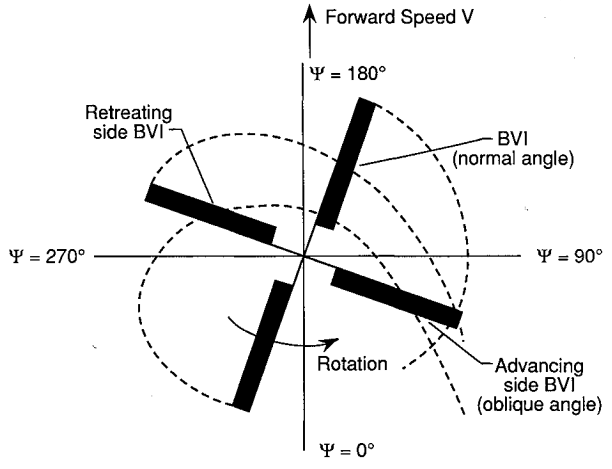

Fig. 1 Blade and vortex positions in forward flight.

Received Nov. 20, 1991; revision received Nov. 12, 1993; accepted for publication Nov. 19, 1993.

*Head, Aeroacoustics Branch, Acoustics Division. Associate Fellow AIAA.
†Senior Research Scientist, Aeroacoustics Branch, Acoustics Division. Member AIAA.
‡Assistant Head, Aeroacoustics Branch, Acoustics Division. Associate Member AIAA.

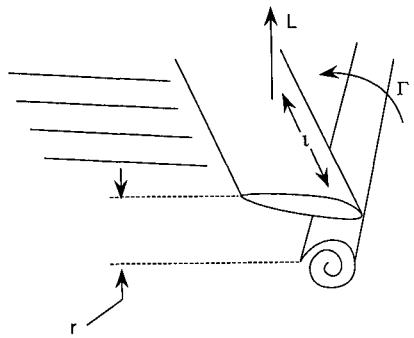

Fig. 2 Schematic showing key parameters for BVI.

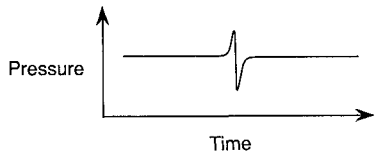

Fig. 3 Calculated BVI noise signature.

although such normal interactions are apparently not important to the BVI noise production. A retreating side BVI is also illustrated.

Although a rigorous prediction of the BVI noise-generating phenomena is not yet possible, advances are being made in numerical simulations of BVI noise. Reference 14 discusses some of the more recent methods. Nevertheless, much can be understood about BVI from simple models. For example, based on analysis of a simplified two-dimensional, shock-free physical model, Hardin and Lamkin[10] found the controlling parameters for BVI noise to be the following: 1) the incoming vortex circulation strength Γ; 2) the portion of the blade span over which two-dimensional (parallel) interaction occurs l; 3) the vortex miss distance r; and 4) the lift L on the blade at the time of the interaction. Figure 2 presents a simple diagram illustrating these parameters for a single interaction. The figure shows a near parallel interaction with the vortex passing beneath the blade. A typical BVI noise signature resulting from a single interaction for an observer below the rotor plane was calculated and is presented in Fig. 3. Note that the signature consists of a positive peak followed by a somewhat larger negative peak. As shown in this article, the effects of multiple interactions produce a much different signature in the far field. Although the calculated result from such a simplified analysis cannot predict the measured result, the physical insight derived from such an analysis has proven useful in both explaining the trends of BVI far-field directivity as well as suggesting means for its control.

BVI Noise Directional Characteristics

The studies performed jointly by NASA Langley and the German Aerospace Research Establishment, DLR, produced a unique and comprehensive data base that documents the BVI impulsive noise character and directionality as functions of rotor flight conditions. The following results are documented in more detail in Ref. 12.

Test Description

Wind Tunnel

The experiments were performed in the open test section of the DNW. The facility is a large, subsonic, atmospheric closed circuit tunnel with open and closed test sections and is located in the Northeast Polder, The Netherlands. The open jet configuration utilizes an 8- by 6-m nozzle that provides a freejet to the test section, which is 19 m in length and is surrounded by a large anechoic room of about 23,000 m^3 with absorptive acoustic wedges. The maximum tunnel speed is about 80 m/s. The background noise levels are low, an ideal condition for aeroacoustic testing.[15]

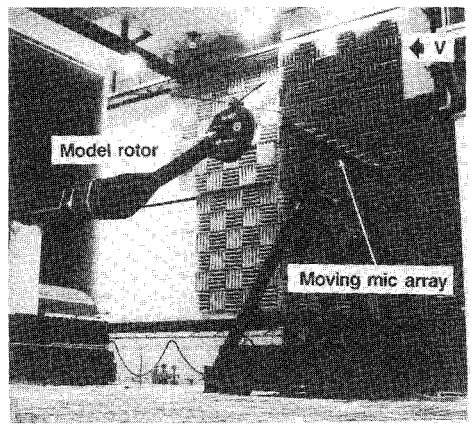

Fig. 4 Photo of model rotor in DNW.

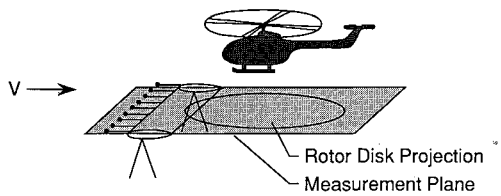

Fig. 5 Sketch depicting acoustic measurement plane.

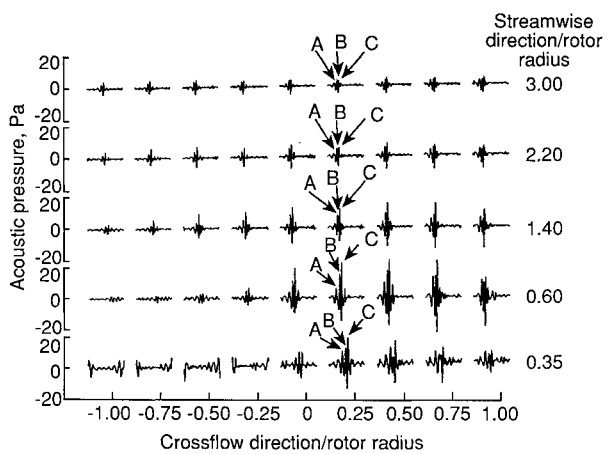

Fig. 6 BVI time histories showing multiple impulses A, B, and C (μ = 0.115; α_{TPP} = 3.4 deg).

Model Rotor

The rotor was a 40% scale, dynamically scaled model of a four-bladed, hingeless B0-105 main rotor. A photograph of the rotor mounted in the DNW open test section is presented in Fig. 4. The rotor had a diameter of 4 m with an NACA 23012 airfoil cross section. The nominal rotor operating speed was 1050 rpm, which resulted in an acoustic blade-passage-frequency of about 70 Hz, a nominal rotor tip speed of 218 m/s, and a hover tip Mach number of 0.64.

Acoustic Instrumentation

The acoustic instrumentation consisted of nine microphones placed in a linear array on a traversing system and two fixed microphones mounted on the fuselage. The nine-element array and traversing system can be seen in Fig. 4. The array microphones were arranged symmetrically with respect to the tunnel centerline, spaced 0.54 m apart, 2.3 m below the rotor hub. The traversing system allowed movement of the microphones both upstream and downstream of the rotor hub.

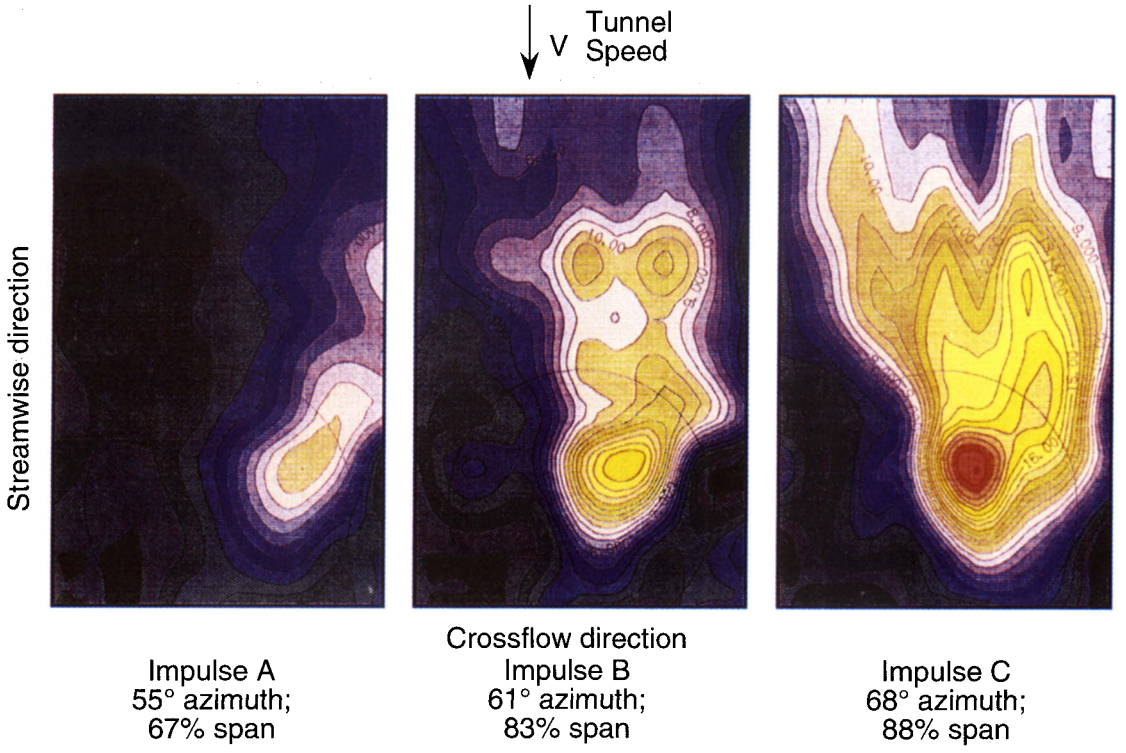

Fig. 7 Directivity of peak values (normalized to a 4-m reference distance to nominal BVI sources) for impulses A, B, and C.

Data Analysis

Utilizing a blade position reference (once-per revolution) signal, 40 rotor revolutions of the raw acoustic signals were digitized and then bandpass-filtered to remove low-frequency loading and thickness noise and high-frequency broadband noise. This process resulted in acoustic time histories dominated by BVI noise in the midfrequency range (500–3000 Hz). To obtain directivity patterns in a large plane beneath the rotor, peak amplitude values from each microphone in the array for a series of array positions both upstream and downstream of the rotor hub were used (Fig. 5). The peak levels were corrected to account for effects of spherical spreading to nominally located BVI sources as described in Ref. 10.

Results

Multiple BVI

The bandpass-filtered time histories of the nine-microphone array at five traverse locations are presented in Fig. 6. The time histories correspond to one representative blade passage for an advance ratio μ of 0.115; a rotor tip-path-plane angle α_{TPP}, of 3.4 deg; at a thrust coefficient C_T of 0.0044. All measurements were upstream of the rotor hub and show three distinct impulsive events A, B, and C measured under the advancing side. The time histories were inspected to identify the peak amplitude and arrival time of each individual impulse over the entire measurement plane. Acoustic triangulation[11] (considered valid at low speed conditions where linear acoustic behavior occurs) was used to estimate the locations of each of the three impulses on the rotor disk. The peak amplitudes in pascals of each impulse were then normalized to a reference distance of 4 m. The resulting directivity patterns are shown in Fig. 7.

Impulse A is the earliest detectable BVI impulse, and was attributed to an interaction at about 55-deg rotor azimuth. This impulse has the lowest acoustic level and radiates in a lobe forward and to the right of the flight path. Impulse B, near 61-deg azimuth, shows higher acoustic levels and radiates more in a forward direction. Impulse C, created at 68-deg azimuth, has the highest noise levels and radiates nearly directly forward. These patterns suggest that the noise source location on the rotor disk has an important effect on the resulting directivity pattern. Recall from Fig. 1 that multiple interactions can occur, and that the BVI angle is dependent on which vortex system is interacting. It has been shown in Ref. 16 that in addition to local Mach number, blade-vortex angle affects BVI noise directionality, which explains the shift in far-field BVI pattern with changing BVI location on the rotor disk.

Effect of Tip-Path-Plane Attitude

BVI directivity patterns based on filtered, averaged, rms sound pressure were determined for different advance ratios for a number of tip-path-plane angles. Whereas, Fig. 7 presented the peak values of specifically identified impulses, this approach quantifies the noise of all BVI impulses generated by the rotor. Figure 8 presents the variation of patterns with tip-path-plane angle at an advance ratio of 0.15. Two primary lobes are observed: 1) one under the advancing side of the rotor, and 2) the other under the retreating side. The BVI lobe from the advancing side interactions starts with a moderate level upstream of the rotor at $\alpha_{TPP} = 0.6$ deg. As tip-path-plane angle increases (increasing descent rate), the lobe moves to the right of the flight path, and the acoustic levels increase. The lobe finally moves off the measurement plane at $\alpha_{TPP} = 6.5$ deg.

The results given here show that the measurement locations were not far enough downwind to completely define the retreating side BVI radiation lobe. The maximum downwind location of the microphone array was limited by interference with the sting, and by the increasing proximity to the lower shear layer of the open jet test section. However, the patterns for the 0.15 advance ratio indicate that the retreating side downwind lobe intensity and directivity are very sensitive to changes in tip-path-plane angle. The levels of the retreating side BVI seem to be nearly as intense as that radiated from the advancing side. Retreating side BVI lobes were also evident in the patterns of the remaining test conditions, but were not sufficiently defined to make more specific conclusions.

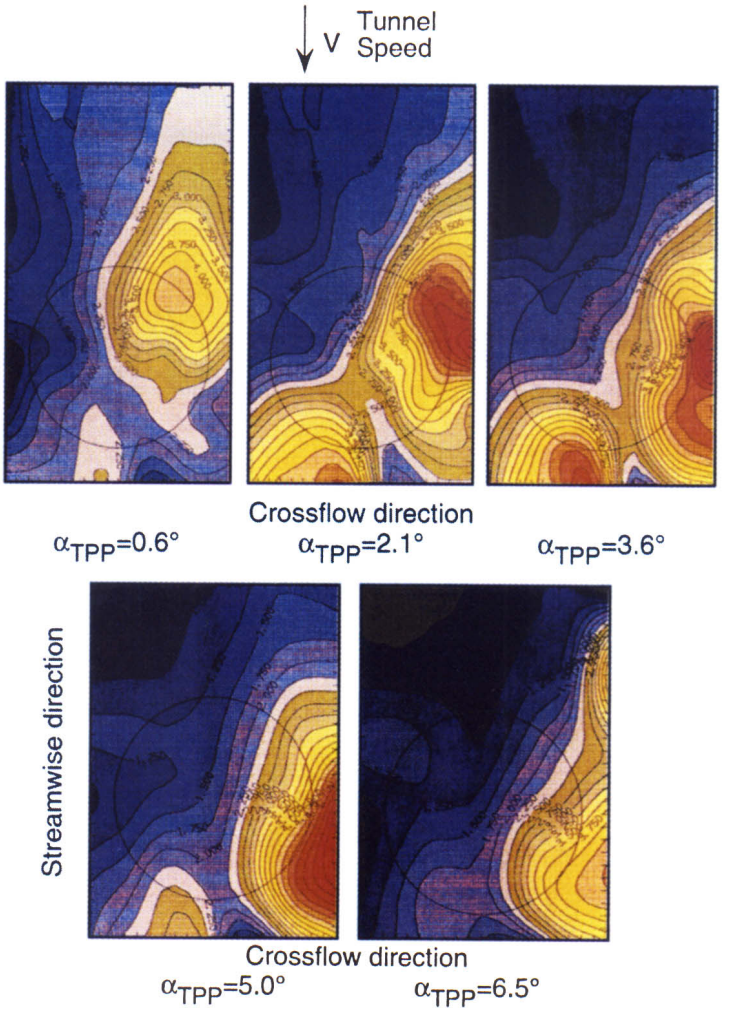

Fig. 8 Variation of BVI noise directivity with tip path plane angle (μ = 0.15).

Source Locations

Free wake geometry predictions from a comprehensive rotor analysis code (CAMRAD/JA) were used to estimate the most likely BVI regions, as explained in Ref. 12. The results for α_{TPP} = 3.6 deg and μ = 0.15 are presented in Fig. 9 along with the directivity contour plot from Fig. 8. Four different symbols are used to differentiate between encounters with the tip vortices of the four different blades. The occurrences are not at the individual symbol locations shown, but over finite regions encompassing clusters of symbols. Symbol placement in the plot is dependent on the 15-deg resolution limitation of the analysis with regard to both blade and vortex positioning. The sizes of the symbols are scaled with each vortex's predicted vertical "miss distance" r (see Fig. 2), with the largest symbols being the closest interactions. The open symbols signify the vortex passing under the blade; the solid symbols signify those passing above the blade.

The primary advancing side interactions are probably due to vortex 1 (circles), vortex 3 (diamonds), and vortex 4 (triangles), all near the 60-deg azimuth line. Vortex 4 is passing from above to below the blades when it is near 60-deg azimuth, 80% radius. The primary acoustic radiation direction is considerably to the right of the flight path for this flight condition, and is roughly normal to the 50- or 60-deg azimuth line. The high acoustic levels may be due to the fact that the interactions are occurring near the tip where the local Mach number is high.

The strongest retreating side BVI is due to vortex 1 (circles), near 300-deg azimuth, 80% radius. Moderate BVI acoustic levels are measured under the aft retreating side of the rotor, in a direction approximately normal to 300-deg azimuth.

The free-wake calculations were used to estimate the interaction locations for test conditions at several other advance ratios, with consistent correlation between the general azimuthal location of the strongest interactions and the general direction of the strongest acoustic radiation. The wake geometry results show that increasing rotor disk angle (tilting "nose up") causes the general region of BVI to move downstream on the rotor disk, causing the interactions to occur at earlier azimuth angles, and therefore, causing the noise to radiate more to the right and downstream of the rotor flight path. The comparison of the BVI location regions with the acoustic directivity patterns clearly supports the conclusion that the BVI noise source radiates most strongly in a direction roughly normal to the blade span.

Blade-Vortex Interaction Noise Control

The following results are from a test designed to evaluate the BVI noise reduction benefit of higher harmonic pitch control, and are documented in more detail in Ref. 13. The principle of this noise control is illustrated in Fig. 10. Recall that BVI noise generation was found to increase with vortex strength and blade lift (that is proportional to blade pitch) at the time of interaction.[10] Pitch control not only modifies blade lift, but also modifies the strengths of the shed vortices and the interaction locations. The amplitude and phasing of such pitch controls may be expected to be important to the noise problem, since the strongest BVI occurrences tend to be lo-

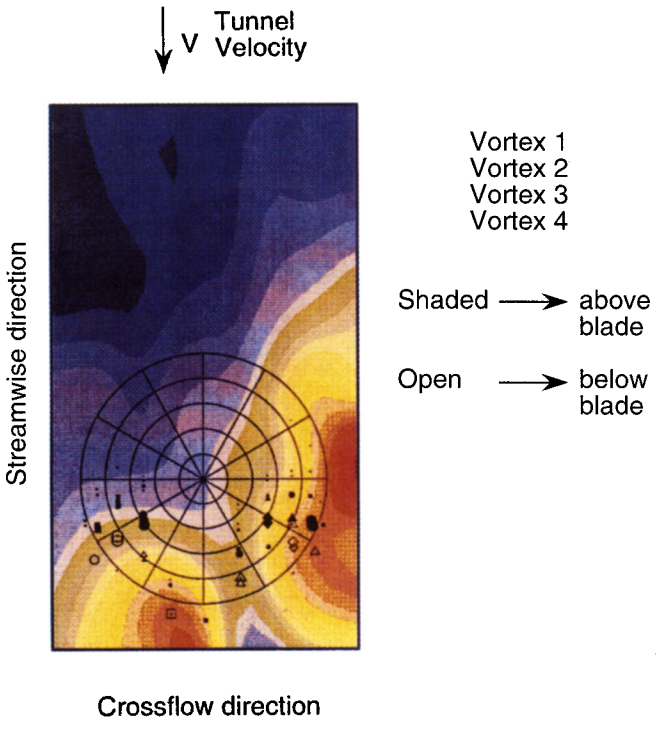

Fig. 9 Predicted BVI regions (μ = 0.15; α_{TPP} = 3.6).

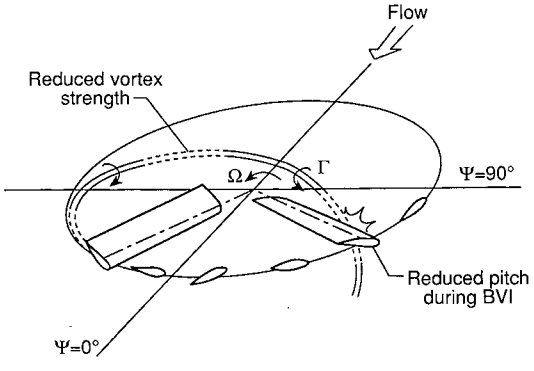

Fig. 10 Illustration of noise reduction concept.

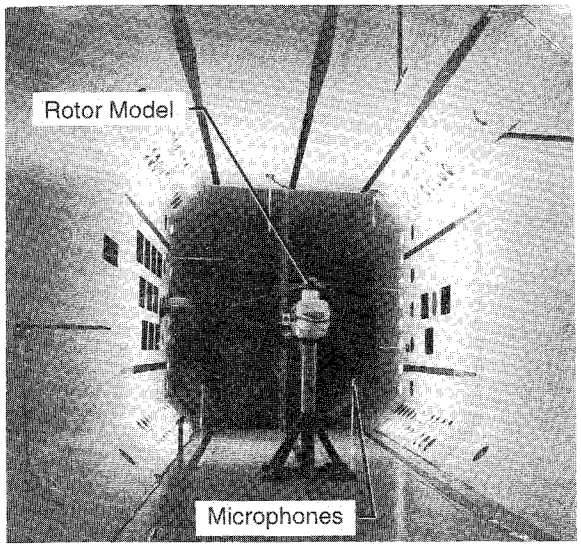

Fig. 11 Photo of model rotor in TDT (arrows show microphones of interest).

cated within a limited azimuth angle range of the first rotor quadrant.

Test Description

Wind Tunnel

The TDT at Langley is a closed-circuit, hard-walled, wind tunnel with a 16-ft-square test section, with either air or Freon-12 used as the test medium. Freon was used for this test since the model rotor was dynamically scaled for operating in this medium, and test Reynolds numbers were higher (closer to full-scale). Because of the freon medium, matched Mach number conditions are achieved with lower rotor and tunnel speeds.

Model Rotor

The test was conducted using the Aeroelastic Rotor Experimental System (ARES). A photograph of the model setup in the wind tunnel is shown in Fig. 11. The rotor had four blades of 2.165 m radius using an untwisted NACA 0012 airfoil section with a 10.77-cm chord. The rotor rotational speed was 650 rpm (the hover tip Mach number was nominally 0.62).

The model rotor was capable of higher harmonic pitch control in the following manner. Blade pitch motion is applied to the rotor through swashplate motions due to three hydraulic actuators. For this four-bladed rotor, the higher harmonic pitch is achieved by superposition of 4/rev ($4P$) swashplate motion upon basic fixed swashplate collective and cyclic ($1P$) flight control inputs. Four/rev collective pitch motion is possible (all four blades pitching the same way simultaneously), as are pitch schedules containing $3P$, $4P$, and $5P$ pitch harmonic components, through proper phasing of the $4P$ inputs. A specially developed computer-based, open-loop control system was used to superimpose the higher harmonic pitch signals on the ARES control system. The pitch motion achieved can be described with the aid of Fig. 12, which shows blade pitch angle data vs blade azimuth angle for a specific flight condition. The $4P$ higher harmonic pitch portion (obtained by subtraction of the total from the baseline case) is seen at the bottom of the figure. The net pitch is not purely a $4P$ collective, but contains other harmonics due to normally occurring pitch-flap and pitch-lag couplings. For the $4P$ collective noise data shown here, the higher harmonic collective pitch amplitude θ_c at azimuthal angle Ψ_c in the first quadrant ($0 < \Psi_c < 90$ deg) is defined in the manner shown in Fig. 12.

Acoustic Instrumentation

Twelve one-quarter-in.-diam pressure-type microphones were used, fitted with nose cones and mounted in vibration isolated streamlined microphone stands. A special calibration scheme[13] was devised and a scaling analysis was made to address the issue of acoustic measurements in a test medium other than air.

Data Analysis

Because of the reverberant (acoustically diffuse) nature of the test section, directivity measurements are not free field and are contaminated by reflections. Hence, a sound power approach was used for data analysis. For the limited data presented here, signals from three of the microphones were used. The microphone signals were analog bandpass-filtered between 200–1600 Hz (3 dB down at 4.5 and 37 blade passage harmonics) to emphasize the impulsive BVI-dominated portion of the noise. The sound pressure levels for each microphone were averaged on a pressure squared basis to obtain a single dB value for each test point. Although little meaning is attached to the absolute dB values, the relative levels and trends of the following results are accurate. This has been verified by subsequent sound power analysis using all 12 microphones.[17]

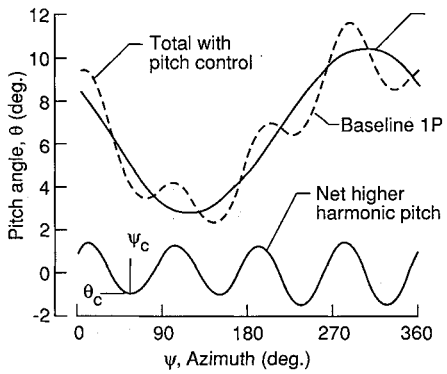

Fig. 12 Blade pitch angle θ vs azimuth angle Ψ for $\mu = 0.266$ and $\alpha_{TPP} = 0$ deg. Pitch control is 4P collective with $\theta_c = -1.0$ deg and $\Psi_c = 60$ deg.

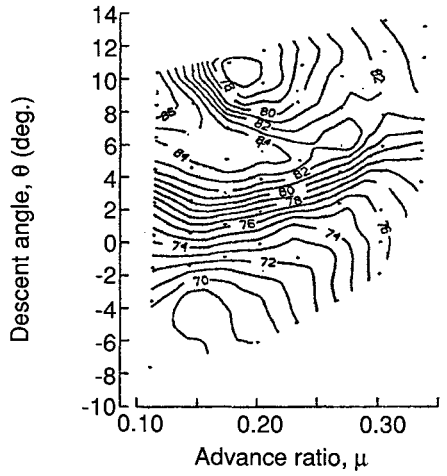

Fig. 13 Noise level (dB) contours for different flight conditions for the baseline (no control) case.

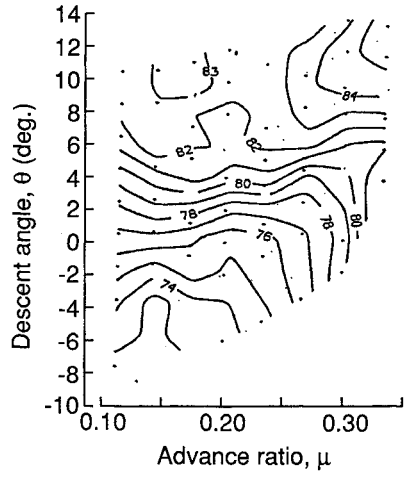

Fig. 14 Noise level (dB) contours for different flight conditions for the 4P pitch control case ($\theta_c = -1.0$ deg; $\Psi_c = 60$ deg).

Results

The rotor was tested over a broad range of operating conditions where the rotor C_T was maintained at 0.005. Rotor advance ratios μ less than 0.11 were not possible due to wind-tunnel minimum operating speed limitations. In order to interpret the noise results in terms of full-scale flight conditions, equivalent flyover descent angles Θ were calculated based on the parasite drag of a typical helicopter.

A key objective of the test was to define flight regimes for which higher harmonic pitch control can be used to reduce BVI noise. Figure 13 shows, for the baseline (no control) case, a contour map of noise levels for a broad range of "full-scale helicopter" descent angles Θ and μ. The contours were generated from the data measured at each point marked on the figure.

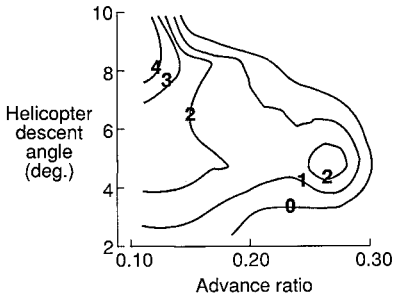

Fig. 15 BVI noise reduction due to higher harmonic pitch control.

Similar data were also obtained for a particular 4P pitch control of $\theta_c = -1$ deg and $\Psi_c = 60$ deg. Figure 14 shows the contour plot for the resultant levels. The effect on the noise is dramatic since the particularly intensive BVI noise region at low advance ratio and high descent angle is eliminated. Figure 15 shows the relative change between the levels of Fig. 14 and that of Fig. 13. Noise reduction is seen to be limited to the landing approach flight regime where BVI noise is most important. The maximum net reduction was 4.7 dB at $\Theta = 8.5$ deg and $\mu = 0.11$. When higher harmonic control is employed (for this particular pitch control, or at other phases and amplitudes), noise tends to increase where BVI is not dominant; i.e., for climb, level flight, steep descent, and high-speed flight for all angles.

Summary

Much progress has been made in recent years on the understanding of BVI noise generation, radiation, and control. Through a simple, two-dimensional analysis, noise generation was shown to depend on four parameters: 1) the incoming vortex strength, 2) the blade lift, 3) the blade span length over which the interaction occurs, and 4) the blade-vortex miss distance. Model rotor wind-tunnel experiments have found BVI noise to be highly directional and extremely sensitive to rotor advance ratio and disk attitude. A rotor free wake analysis demonstrated the likelihood of multiple BVI, as observed in the measurements. In addition, the measured peak radiation direction was consistent with both the simple analysis and the predicted interaction regions on the rotor disk. Moreover, the knowledge gained through the analysis and wind-tunnel results suggested a means of BVI noise control, namely higher harmonic pitch control. A sound power experiment performed in a hard-walled tunnel clearly demonstrated that sound power reduction was possible for rotorcraft operation conditions typical of landing approach. BVI noise reductions appeared to correspond to reductions in blade lift (pitch) and vortex strength in the vicinity of BVI encounters.

References

[1]Boxwell, D. A., and Schmitz, F. H., "Full-Scale Measurements of Blade Vortex Interaction Noise," *Journal of the American Helicopter Society*, Vol. 27, No. 4, 1982, pp. 11–27.

[2]Charles, B. D., "Acoustic Effects of Rotor-Wake Interaction During Low-Power Descent," American Helicopter Society Symposium on Helicopter Aerodynamic Efficiency, May 1975.

[3]Tangler, J. L., "Schlieren and Noise Studies of Rotors in Forward Flight," American Helicopter Society, AHS Paper 77.33-05, May 1977.

[4]Splettstoesser, W. R., Schultz, K. J., Boxwell, D. A., and Schmitz, F. H., "Helicopter Model Rotor-Blade Vortex Interaction Impulsive Noise: Scalability and Parametric Variations," NASA TM-86007, Dec. 1984.

[5]Hoad, D. R., "Helicopter Model Scale Results on Blade-Vortex Interaction Impulsive Noise as Affected by Tip Modification," American Helicopter Society, AHS Paper 80-62, May 1980.

[6]Martin, R. M., and Connor, A. B., "Wind Tunnel Acoustic Results of Two Rotor Models with Several Tip Designs," NASA TM-87698, July 1986.

[7]Schlinker, R. H., and Amiet, R. K., "Rotor Vortex Interaction Noise," NASA CR 3744, Oct. 1983.

[8]Hubbard, H. H., "Aeroacoustics of Flight Vehicles: Theory and Practice," NASA RP-1258, Vol. 1; WRDC TR 90-3052, Aug. 1991.

[9]JanakiRam, R. D., "Aeroacoustics of Rotorcraft, Aerodynamics of Rotorcraft," AGARD R781, May 1990.

[10]Hardin, J. C., and Lamkin, S. L., "Concepts for Reduction of Blade/Vortex Interaction Noise," *Journal of Aircraft*, Vol. 24, No. 2, 1987, pp. 120–125.

[11]Martin, R. M., Splettstoesser, W. R., Elliott, J. W., and Schultz, K. J., "Advancing Side Directivity and Retreating Side Interactions of Model Rotor Blade Vortex Interaction Noise," NASA TP-2784, May 1988.

[12]Martin, R. M., Marcolini, M. A., Splettstoesser, W. R., and Schultz, K. J., "Wake Geometry Effects on Rotor Blade-Vortex Interaction Noise Directivity," NASA TP-3015, Nov. 1990.

[13]Brooks, T. F., Booth, E. R., Jr., Jolly, J. R., Jr., Yeager, W. T., Jr., and Wilbur, M. L., "Reduction of Blade-Vortex Interaction Noise Through Higher Harmonic Pitch Control," *Journal of the American Helicopter Society*, Vol. 35, No. 1, 1990, pp. 86–91.

[14]Hassan, A. A., Tadghighi, H., and Charles, B. D., "Aerodynamics and Acoustics of Three-Dimensional Blade-Vortex Interactions," NASA CR-182026, July 1990.

[15]Van Ditshuizen, J. C. A., Courage, G. D., Ross, R., and Schultz, K.-J., "Acoustic Capabilities of the German-Dutch Wind Tunnel DNW," AIAA Paper 83-0146, Jan. 1983.

[16]Widnall, S., "Helicopter Noise Due to Blade-Vortex Interaction," *Journal of the Acoustics Society of America*, Vol. 50, No. 1, Pt. 2, 1971, pp. 354–365.

[17]Brooks, T. F., and Booth, E. R., Jr., "Rotor Blade-Vortex Interaction Noise Reduction and Vibration Using Higher Harmonic Control," 16th European Rotorcraft Forum, Paper 9.3, Sept. 1990.